Songklanakarin J. Sci. Technol.
44 (4), 1085–1090, Jul. – Aug. 2022

http://www.sjst.psu.ac.th

Original Article

Optimization of a heavy-duty elevated thin shell structure

Azizah Abdul Nassir[1], Yee Hooi Min[1*], Arthit Petchsasithon[2], and Syahrul Fithry Senin[1]

[1] *Centre for Civil Engineering Studies, Universiti Teknologi MARA, Cawangan Pulau Pinang, Permatang Pauh Campus, Pulau Pinang, 13500 Malaysia*

[2] *Department of Civil Engineering, King Mongkut's Institute of Technology Ladkrabang, Yannawa, Bangkok, 10120 Thailand*

Received: 8 February 2022; Revised: 5 May 2022; Accepted: 1 June 2022

Abstract

Optimization means the mathematical determination of the optimal decisions out of diverse alternatives. Based on the preceding Finite Element Analysis (FEA), a proposed shell produced a maximum stress that exceeded the design value. To make the design feasible, an optimization was done to minimize the maximum stress by using the gradient method. The performance of the structure can be optimized to fulfil the design requirements with the optimum value of displacement to achieve the objective function. The results show that the optimum displacement is 8.8mm, which reduced the maximum stress by 99.94% from the initial level. Thus, optimization methods are important for new applications of shell structures to find their best parameters in the design stage.

Keywords: thin shell structure, finite element analysis, maximum stress, optimization, displacement

1. Introduction

Thin shell structure applications in building construction are limited to the roof component. In designing a shell structure, an optimum geometrical design will provide huge advantages for membrane stress in allowing to achieve an efficient system of load bearing (Pereira, 2015). A common shell structure optimization aim was to reduce the weight of the shell, to keep it lightweight while maintaining the maximum stress that does not exceed the structure's limit to prevent failures (Gil-Ureta, Pietroni, & Zorin, 2019). Optimization has become an effective tool among the various techniques of form-finding for shell structures, deciding on optimal parameters by computational mechanics. Improvements of a structure's mechanical behavior can be achieved by using shape optimization even with minor changes to the structural geometry (Tomas & Marti, 2010).

A study has been done on a thin glass fiber reinforced polymer (GFRP) with two different types of geometries, which are oblate and prolate domes. The study has taken three approaches to compare the failure results, which are through analytical approach, numerical analysis, and experimentally. Based on the results, it was found that all the three methods of study came out in mutual concordance for oblate domes, but got discordant results for the prolate dome. The stress deformation concentrated more at the boundaries rather than being uniformly distributed through the surfaces, due to different surface regions and stacking. The study concluded that the stress failure can be minimized by identifying the exposed failure areas for strengthening purposes (Gohari, Sharifi, Burvill, Mouloodi, Izadifar, & Thissen, 2019).

In data validation of analysis, a study has been carried out to compare the Finite Element (FE) analysis output with the analytical solution. The study was modelling some composite plates for electro-mechanical coupling. The mesh convergence analysis was carried out to minimize the error by finding the optimum density of mesh. The findings indicated that the finite element analysis gave output closely similar with the analytical calculations. There are four cases with different meshes, each having a different number of piezoelectric patches, which are 1250 for case 1, 272 for case

*Corresponding author
Email address: minyh@uitm.edu.my

2, 180 for case 3 and 1250 for case 4. Based on the output, case 2 obtained the largest error at 9.09% followed by case 3 with 8% of error. Case 1 got the least error at 6.06% followed by case 4 with 7.89% of error. However, the paper suggests adding another method to improve measuring the error, such as using artificial neural network and machine learning (Gohari, Mozafari, Moslemi, Mouloodi, Sharifi, Rahmanpanah, & Burvill, 2021).

In this study, a shape optimization has been done for a shell structure to make the proposed shell structure feasible by reducing the maximum stress to a lesser value, so it becomes allowable. The model has been adopted in a previous study, where the load applied was a heavy loading to resist building throughout the shell's surface (Abdul, Hooi, Fithry, & Yian, 2020). This model was proposed to be one of the alternatives to become an elevated platform as an existing high place for residential building, located at a common flood area. Unfortunately, the pendentive geometry is one of the shapes proposed that produce a higher maximum compressive stress than the design value of material, namely its characteristic strength, f_{ck}.

Figure 1 shows the equivalent resultant von Mises stress, and N_e contour of the pendentive thin shell structure. With a constant shell thickness of 0.3m, the maximum value of equivalent resultant stress is 102.89 MN/m, with the maximum stress at 342.97 N/mm^2 which is much greater than the design value of material strength, 40 N/mm^2. The validation of data in this paper applied mesh convergence test to determine the percentage of error in the optimization of the shell. Thus, the findings in this study improved the maximum stress of the proposed shell structures by minimizing the stress, by finding the optimum value of the displacement.

2. Thin Shell Structure Modelling

Modelling for a complex geometry usually uses the finite element method, a numerical method, as solution for the problem cannot be obtained analytically. It is applied to understand the behavior of complex objects and to predict the performance of a design, with a high accuracy. In this section, the equation for pendentive geometric modelling has been evaluated and the model parameters are described in detail.

2.1. Pendentive shell structure formulation

Pendentive shape is initially a combination of a virtual cube with a sphere. The center node of sphere is located at the cube's axis, making the diameter related to the center of the cube (Elkhateeb, 2012). An illustration of the geometric combination is shown in Figure 2. In this study, the pendentive geometry was generated by the combination of square with a spheroid. The general equation for spheroid in Cartesian coordinates is as in Equation 1 (Poelaert, Schiewind & Janssens, 2011). The parameters in the equation represent radius of the spheroid, R, azimuth angle, φ and polar angle, θ, which satisfy $0 \le \varphi \le 2\pi$ and $0 \le \theta \le \pi$. Meanwhile, a and c are positive numbers where the axes in directions {x, y} and z intersect with the spheroid.

$$\begin{aligned} &\text{x-coordinate} = a \sin\theta \sin\varphi \\ &\text{y-coordinate} = a \sin\theta \cos\varphi \\ &\text{z-coordinate} = c \cos\varphi \end{aligned} \quad (1)$$

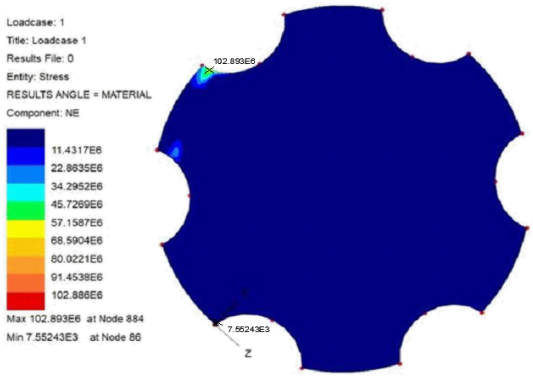

Figure 1. Equivalent resultant von Mises stress contour of proposed pendentive shell structure (Abdul *et al.*, 2020)

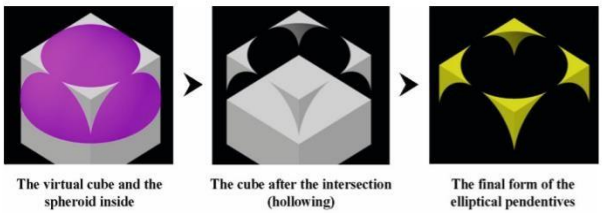

Figure 2. Development of pendentive geometry using spheroid (Elkhateeb, 2012)

As this spheroid has the same semiaxes a=b, for intersections with the axes x and y, the radius of the spheroid at any point can be expressed as in Equation 2 (Elkhateeb, 2012). The variables must satisfy the conditions $-\pi/2 \le \gamma \le \pi/2$ and $0 \le \lambda \le 2\pi$ where γ is the latitude and λ is the longitude.

$$R = \frac{abc}{\sqrt{c^2(a^2\cos^2\lambda + a^2\sin^2\lambda)\cos^2\gamma + a^2b^2\sin^2\gamma}} \quad (2)$$

Pendentive geometry has got several hollow parts near the boundary also known as the "transitional zone" to eliminate the unwanted blocks formed by the cube during the combination of the geometries. This part was justified by architects and engineers during the revolution of pendentive, to be heavy with no necessary reason to be constructed (Elkhateeb, 2012). To calculate the height of the hollow part of the pendentive, h_h, the general equation is Equation 3 where L is the length of the cube.

$$h_h = \frac{2L}{\sqrt{2}} - L = 0.4142\,L \quad (3)$$

2.2. Shell Structure Parameters and Variables

Shell dimensions are referred to the original model of pendentive proposed since the shell needs a modification by using optimization in this study. It was estimated that a house with 2000 sqft size has a loading of 185,962 kg, equivalent to 9.82kN/m^2. The tested applied load was 20kN/m^2, to consider the surrounding infrastructure of the buildings and for safety factors (Abdul *et. al.*, 2020). The boundary condition of the shell was fixed support, to emulate the real condition in construction application. Due to the

intermittency of lower part of the geometry, the supports are only placed at the enclosed part of the pendentive. The loadings and support assigned are shown in Figure 3. Meanwhile for the material properties, conventional reinforced concrete of a high concrete grade, C40, was chosen with a thin shell element from the material library. Thickness of the shell was tested with 0.3m, classified as a thin shell since it satisfied the condition of radius over thickness, R/t > 20 (Sadowski & Rotter, 2013).

The peak height of the pendentive used is 20 meters, and the diameter of the bottom surface of pendentive is 200 meters. The peak height chosen is considered the maximum flood height in historical data and hydrological calculation design for ARI-100, at the worst location of flood in Malaysia (Abdul *et. al.*, 2020). The height also has been checked for bending limitation of rise to span ratio, $1/10 > h/d < 1/6$ (Maten, 2011). The mesh for interpolation of analysis in the modelling is set to be non-uniform in size throughout the surface geometry. In the finite element analysis, stresses generated are based on von Mises criterion used to determine the fracture or yield limitations of a structure or material given (Sica, 2018). The complete model of pendentive thin shell structure is shown in Figure 4.

3. Relationship Between Stress and Displacement

Stress and displacement have affected the behavior of the structure since the displacement increases with stress. The yield point represents the start of the structure failing, where it has reached the maximum displacement and is no longer able to resist the stresses (Wang & Wang, 2012). In this case, the original model has produced a higher maximum stress than the material yield point. Hence, the material has reached its plastic region beyond the failure point. The elasticity of the structure depends on the material Young's modulus, E, that can be obtained from the slope of load vs. displacement. Even though stress and displacement can be independent from each other, stress is producing a strain deformation and the curve of stress vs. strain is obtained from the relationship of force vs. displacement (Wang, Shi, & Wang, 2017). This is because the strain is calculated based on the percentage of changes in the material displacements.

Displacement is also an important factor in determining material limitations in analysis. It's conceivable that the displacement exceeds required values for workability and safety, or that the overall dissipation reaches a point where the material fails (Donmez *et al.*, 2012; Palladino *et al.*, 2020). The general force vs. displacement plot is shown in Figure 5.

4. Optimization

Generally, structural optimization requires three main formulations, which are objective function, state variables, and design variables. The aim of an optimization should be included in the objective function, f, either to be maximized or minimized. The designations of the structure, such as thickness, height, or geometry of the shell, should be considered in formulation of the design variable, x. Meanwhile the responses to the optimized values, such as stress, displacement and mass of structure, are represented in the state variables, y (Larsson, 2016). To solve the objective

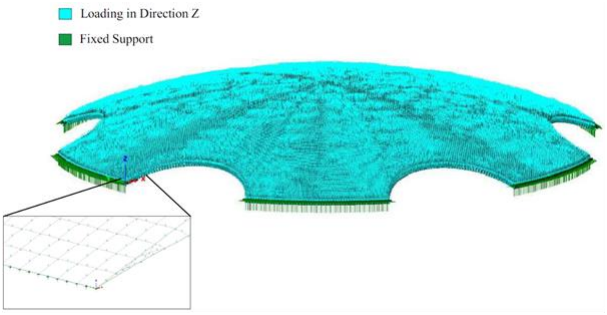

Figure 3. Illustration of load applied throughout the shell surfaces and supports at the shell boundary condition

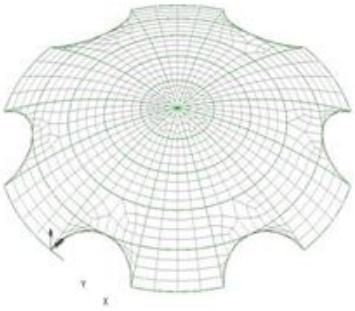

Figure 4. Modelling of pendentive elevated thin shell platform

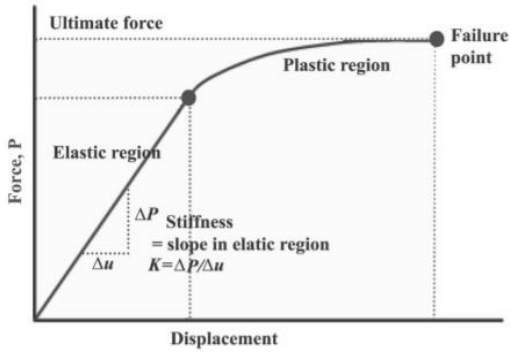

Figure 5. Graph of force vs. displacement (Donmez et al., 2012)

function, the optimization is subjected to the state and design variables, while the state variables depend on the variables of the design, y(x). This method has been proven to be closer to the final design of engineering, to be less time consuming, and comparatively simple on solving complicated optimization problems (Holmberg, Torstenfelt, & Klarbring, 2013). Thus, the general simultaneous equation for the optimization is stated in Equation 4 (Larsson, 2016).

$$\begin{cases} Min_x & f(x, y(x)) \\ \text{Subject to} & \begin{cases} \text{Design constraint on x} \\ \text{State constraint on y(x)} \\ \text{Equilibrium constraint} \end{cases} \end{cases} \quad (4)$$

In this study, the objective is to minimize the maximum equivalent resultant stress, with two proposed state variables which are nodal displacements of the shell. This optimization formulation is suitable for solving complex optimization problems with the von Mises stress values that

employ multi-dimensional models. The design constrains used are the height and the span of the shell, to control the bending resistance of the pendentive. Therefore, the structure of the optimization is as shown in Table 1. In this study, the software used for the optimization is HyperMesh due to the high efficiency and quality of meshing ability which aids in solving a variety of complex finite element modelling problems. It also offers good grid processing with a better finite element pre-processing function (Sinian & Anping, 2018).

Table 1. Summary of optimization input

Objective function, f	Design variable, x	State variable, y
Minimize the maximum stress	Height, Span	Displacement

5. Results and Discussion

5.1. Shape optimization on pendentive shell

The model was run for optimization and several iterations have been generated. The iteration of optimization output is as tabulated in Table 2 and the trend of the output is drawn in Figure 6. Values for displacement have been changed to a positive number in the graph due to the sign referring to the nodal movement direction. Based on the output in Table 2 and Figure 6, the results have show the optimum value of nodal displacements to achieve the minimum of maximum equivalent resultant stress. The optimum displacement is at iteration 21, with a reading of 0.0088m (downward) and the least maximum equivalent resultant stress is 0.6669 x10^5 N/m. To convert the equivalent resultant stress to maximum stress, a calculation employed equation (5):

$$\sigma_{\max} = \frac{N_e}{t} \tag{5}$$

(John, 1999) where t is the thickness of the pendentive, and N_e is the maximum equivalent resultant stress. Taking t = 0.3m, the new maximum stress after optimization is 0.222N/mm^2 which is less than the allowed design value of C40 concrete, 40N/mm^2. The value of maximum stress has been reduced by about 99.94% compared to the initial one before optimizing the model.

5.2. Mesh sensitivity analysis

The convergence test is critical for solutions obtained from FEM analysis to evaluate the reduction of error during refining the finite element mesh. In this study, the justification of error for FEM output is measured using relative error and mesh sensitivity analysis. The meshing description has assigned a thin shell structural element type with quadrilateral element shape. Therefore, the interpolation order chosen was quadratic to be compatible in solving the chosen element shape. The mesh density modelling is shown in Figure 7, in which the mesh assignments were iterated with three densities starting from a dense mesh, medium mesh, and coarse mesh with irregular element patterns.

Table 2. Iteration of optimization output

Iteration	Variable	
	Maximum displacement, m	Maximum equivalent resultant stress, x10^5 N/m
0	-0.0202058	2.10417
1	-0.0917481	0.929657
2	-0.00835819	0.929657
3	-0.0082729	0.929657
4	-0.0091917	1.08744
5	-0.00968012	0.911319
6	-0.00924362	0.788552
7	-0.00852193	0.71623
8	-0.00809655	0.681821
9	-0.00791729	0.701464
10	-0.00784909	0.667151
11	-0.0080635	0.675701
12	-0.00843242	0.739626
13	-0.00832695	0.700114
14	-0.00822392	0.748243
15	-0.00803997	0.68624
16	-0.0082099	0.667882
17	-0.0083645	0.69177
18	-0.00859973	0.673613
19	-0.00878989	0.676587
20	-0.00897209	0.671383
21	-0.00880081	0.66691
22	-0.00869438	0.66698
23	-0.00887266	0.669372

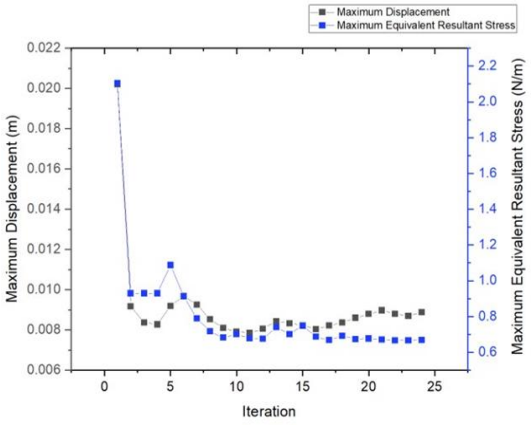

Figure 6. Graph of optimization output, maximum displacement and maximum equivalent resultant stress vs. Iteration

The illustration in Figure 8 shows a clearer picture of the location of element nodes and the directions of the degrees of freedom for the thin shell structure. For the proposed thin shell in a 3-dimensional modelling, the number of nodes is 8 per element, with 5 degrees of freedom that consist of translation in direction X, Tr, translation in direction Y, Ty, translation in direction Z, Tz, node rotation in direction X, Rx, and node rotation in direction Y, Ry. These DOF are important in FE analysis since they control the movement after the loading has been applied, which causes the deformation of structure by displacements and related stresses.

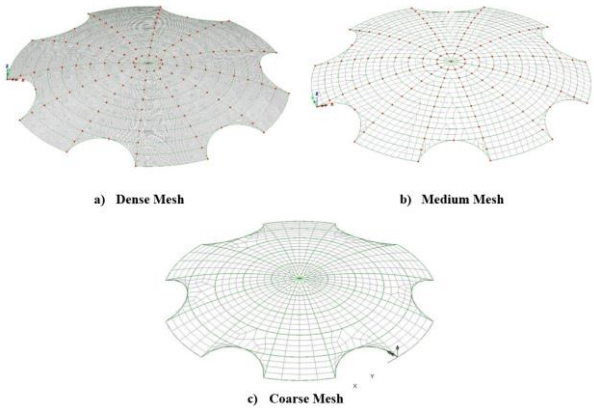

Figure 7. Modelling of pendentive elevated thin shell platform with different mesh densities a) Dense Mesh, b) Medium Mesh and c) Coarse Mesh

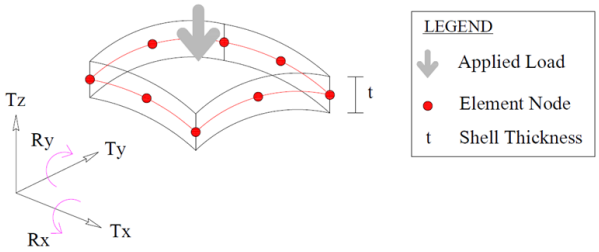

Figure 9. Graph of optimization output, maximum displacement and maximum equivalent resultant stress vs. Iteration

FEM output relative error was used, due to having no exact formula for the stress in 3-dimensional continuum thin shell under heavy loading application in the complex geometry chosen. The data obtained can be assessed for the relative error by calculating the error percentages between three different mesh densities to estimate their accuracy and precision. Equation 6 below was used to calculate the relative error percentage where X_0 is the actual value from the FEM and x is the measured value from varied mesh densities. The computed error, Xr should be less than the specified accuracy for relative error, X_{max} = 5% in quadrilateral element computations (Khan, Abid, Ahmad, Faiz, Memon, Iqbal, & Ming, 2002).

$$Xr = \frac{X_0 - X}{X_0} \quad (6)$$

Based on the calculated results in Table 3 below, the relative errors were all lesser than the accuracy of 5% with only small gaps between all types of mesh. However, the dense mesh shows the least relative error compared to the medium and the coarse mesh discretizations. This shows that the FEM output had insignificant errors with good agreement among the three mesh analyses tested on the pendentive shell. In FEM, the mesh type has a large influence on the output accuracy due to the number of the nodes. A larger number of nodes will lead to a greater accuracy of output and a non-uniform mesh should be applied to vary the solutions (Reddy, 2006). However, a larger number of nodes will cause a more computationally intensive process in solving the analysis for each node. Therefore, an appropriate mesh density should be identified, to minimize/balance these issues and obtain an optimal number of iterations to convergence.

6. Conclusions

To conclude, the proposed pendentive has become feasible for heavy loading application after the optimization. The stresses were reduced by optimizing the displacement value, contributing to a feasible preliminary design phase of the new application of thin shell structure. The findings in this paper can provide a design reference for engineers in deciding the parameters and physical geometry for future implementation of a long span shell structure with heavy duty.

A prior study has come out with a new application of shell structure as the platform for buildings, but when load analysis was carried out the pendentive geometry was not feasible due to the maximum stress exceeding the material design limit. Thus, this paper has successfully optimized the pendentive geometry by finding the optimal displacement of the nodes to minimize the maximum stress, and to make heavy loading application attainable.

The placement of buildings on top of shell surfaces can help reduce the number of flood victims, especially at areas affected during monsoon seasons. Not only by providing an elevated platform, but the construction of shell can also minimize the soil compaction work leaving undisturbed space underneath.

Acknowledgments

This research did not receive any specific grant from funding agencies in public, commercial, or non-for-profit sectors.

References

Abdul, A., Hooi, Y., Fithry, S., & Yian, W. (2020). Sustainable development of elevated shell platform. *Engineering Journal, 25(6),* 123–130. doi:10.4186/ej.2021.25.6.123.

Donmez, B. O., Ozdemir, S., Sarikanat, M., Yaras, N., Koc, P., Demir, N., . . . Oguz, N. (2012). Effect of angiotensin II type 1 receptor blocker on osteoporotic rat femurs. *Pharmacol. Reports, 64(4),* 878–888. doi:10.1016/S1734- 1140(12)70882-4.

Table 3. Results of mesh sensitivity analysis

Mesh type	No. of Nodes	No. of elements	Maximum Equivalent Resultant Stress, σ_{Max} x 10^5 N/m	Percentage of Relative Error, *Xr*
Dense Mesh	28,961	27,284	0.6554	1.7296
Medium Mesh	15,211	14,350	0.6549	1.7977
Coarse Mesh	1,445	1,207	0.6544	1.8678

Elkhateeb, A. A. (2012). Domes in the Islamic architecture of Cairo city: A mathematical approach. *Nexus Network Journal, 14(1),* 151–176. doi:10.1007/s00004-011-0103-3.

Gil-Ureta, F., Pietroni, N., & Zorin, D. (2019). Structurally optimized shells. Retrieved from https://arxiv.org/pdf/1904.12240.pdf

Gohari, S., Mozafari, F., Moslemi, N., Mouloodi, S., Sharifi, S., Rahmanpanah, H., & Burvill, C. (2021). Analytical solution of the electro-mechanical flexural coupling between piezoelectric actuators and flexible-spring boundary structure in smart composite plates. *Archives of Civil and Mechanical Engineering*, 21(1). doi:10.1007/s43452-021-00180-z

Gohari, S., Sharifi, S., Burvill, C., Mouloodi, S., Izadifar, M., & Thissen, P. (2019). Localized failure analysis of internally pressurized laminated ellipsoidal woven GFRP composite domes: Analytical, numerical, and experimental studies. *Archives of Civil and Mechanical Engineering*, 19(4), 1235–1250. doi:10.1016/j.acme.2019.06.009

John, M. (1999). Bending stresses and direct stresses combined, *Strength of Materials and Structures* (pp. 283-294). doi:10.1016/B978-1-4831-9652-7.50060-8.

Khan, Abid, Ahmad, Faiz, Memon, Iqbal, Ming, & Xu. (2002). Error computations for adaptive finite element analysis. *Journal of Engineering and Applied Sciences*, *21*. 53-60.

Larsson, R., (2016). Methodology for topology and shape optimization: Application to a rear lower control arm (Master's thesis, Chalmers University of Technology, Goteborg, Sweden). Retrieved from https://publications.lib.chalmers.se/records/fulltext/238778/238778.pdf

Maten, R. N. (2011). Ultra-high-performance concrete in large span shell structures. (Master's thesis, Delft University of Technology, Delft, the Netherlands). Retrieved from http://homepage.tudelft.nl/p3r3s/MSc_ projects/reportterMaten1.pdf

Palladino, S., Esposito, L., Ferla, P., Totaro, E., Zona, R., & Minutolo, V. (2020). Experimental and numerical evaluation of residual displacement and ductility in ratcheting and shakedown of an aluminum beam. *Applied Science, 10(10).* doi:10.3390/app10103610.

Pereira, V. V. (2015). Design and applications of ultra-thin freeform shell structures. *Extended Abstract Tecnico Lisboa*.

Poelaert, D., Schniewind, J., & Janssens, F. (2011). Surface area and curvature of the general ellipsoid. *Classical Analysis and ODEs (math.CA), arXiv.* doi:10.48550/ARXIV.1104.5145

Reddy, A., C. (2006). Discretization errors in finite element analysis of non-linear 2-D structural problems with large strains and plasticity. *Two-Day National Level Seminar on FEM and Its Application to Non-Linear Problems*. 25-36.

Sadowski, A. J., & Rotter, J. M. (2013). Solid or shell finite elements to model thick cylindrical tubes and shells under global bending. *International Journal Mechanical Science, 74*, 143–153, doi:10.1016/j.ijmecsci.2013.05.008.

Sica, L. U. R. (2017). An experimental study of the validity of the von Mises yielding criterion for elasto-viscoplastic materials. *Pontificia Universidade Catolica Do Rio De Janeiro*, 91.

Sinian, H., & Anping, W. (2018). Finite element analysis of space science experimental equipment based on HyperMesh and Nastran. *MATEC Web Conference, 198*. doi:10.1051/matecconf/201819805010.

Tomás, A., & Martí, P. (2010). Shape and size optimisation of concrete shells. *Engineering Structure, 32 (6),* 1650–1658. doi:10.1016/j.engstruct.2010.02.013.

Wang, M. B., & Wang, G. (2012). A stress-displacement solution for a pressure tunnel with impermeable liner in elastic porous media. *Latin American Journal of Solids and Structures, 9,* 95-110.

Wang, Y., Shi, G., & Wang, X. (2017). Displacement and stress analysis of laminated composite plates using an eight-node quasi-conforming solid-shell element. *Curved Layer Structure, 4(1),* 8–20. doi:10.1515/cls-2017-0002.